U.PORTO

FACULDADE DE MEDICINA DENTÁRIA
UNIVERSIDADE DO PORTO

HYPERLIPIDAEMIA'S IMPACT ON BONE REMODELLING AND DEVELOPMENT: ASSESSMENT IN THE *EX VIVO* ORGANOTYPIC EMBRYONIC CHICK FEMORA MODEL

JOÃO GABRIEL TEIXEIRA CARDOSO

TESE DE MESTRADO INTEGRADO EM MEDICINA DENTÁRIA

FACULDADE DE MEDICINA DENTÁRIA DA UNIVERSIDADE DO PORTO

PORTO, 2021

U.PORTO

FACULDADE DE MEDICINA DENTÁRIA
UNIVERSIDADE DO PORTO

HYPERLIPIDAEMIA'S IMPACT ON BONE REMODELLING AND DEVELOPMENT: ASSESSMENT IN THE *EX VIVO* ORGANOTYPIC EMBRYONIC CHICK FEMORA MODEL

JOÃO GABRIEL TEIXEIRA CARDOSO

TESE DE MESTRADO INTEGRADO EM MEDICINA DENTÁRIA

FACULDADE DE MEDICINA DENTÁRIA DA UNIVERSIDADE DO PORTO

PORTO, 2021

Dissertação apresentada à Faculdade de Medicina Dentária da Universidade do Porto, para obtenção do grau de mestre em Medicina Dentária

Autor

João Gabriel Teixeira Cardoso

Aluno do 5º ano do Mestrado Integrado em Medicina Dentária na Faculdade de Medicina Dentária da Universidade do Porto

up201708486@edu.fmd.up.pt

Orientador

Prof. Doutor Pedro de Sousa Gomes

Professor Associado da Faculdade de Medicina Dentária da Universidade do Porto

Consultor

Mestre Victor Zacharias Martin

Faculdade de Medicina Dentária da Universidade do Porto

Porto, 2021

“Por si só, o tempo não é nada.

A idade de nada é nada.

A eternidade não existe.

No entanto, a eternidade existe.”

José Luís Peixoto

Acknowledgments

À minha mãe, uma guerreira incansável sempre pronta a lutar pelas minhas causas, e ao meu pai, o meu conselheiro sempre presente, por todo o amor, esforço e confiança. Tudo o que tenho e, mais importante, tudo o que sou, tenho e sou graças a vocês. As minhas vitórias serão sempre as nossas vitórias.

Ao Paulo, o meu tio e padrinho de batismo, que sempre esteve, está e estará a meu lado para ver o caminho que tenciono percorrer. Obrigado por teres sido o irmão mais velho que nunca tive. Tenho imensa sorte em poder ter-te conhecido.

Ao Miguel, por ser o companheiro de todas as horas, com quem sempre pude partilhar tudo e que sempre me ajudou a tornar-me, cada vez mais, uma pessoa melhor. Obrigado por seres a minha segunda família.

A todos os educadores, professores e funcionários que olharam por mim durante todos estes anos. Além de todo o conhecimento passado, agradeço-vos a todos pela infindável paciência, pela dedicação, pelo sentido de humor e, no fundo, por todo o carinho. Todo e cada um de vós deixou parte de si em mim.

Ao meu orientador, o Professor Dr. Pedro Gomes, pela forma calorosa com a qual sempre se dirigiu a mim, pela sua supervisão e pela amabilidade, quer em contexto de aula quer durante todo o processo de investigação. Não podia ter feito uma escolha melhor.

Ao Dr. Victor Martin, pela forma incansável com a qual sempre esteve disponível para me prestar auxílio durante as várias fases de redação da presente dissertação. Pelo seu imenso conhecimento e pela sua amabilidade. Tive muita sorte em tê-lo como ajuda.

Ao Sr. Miguel Mendes dos Serviços Académicos da FMDUP, por toda a sua amabilidade.

Ao meu trinómio, por aturarem todos os meus dias maus, por me tentarem ajudar a melhorar em qualquer circunstância apesar das discussões. Obrigado por serem a melhor equipa que poderia pedir.

A todas as amizades que fui colecionando pelo meu percurso académico fora, por me terem ajudado a crescer e a ver o mundo de uma forma diferente. A todos vós sou eterna e infinitamente grato.

Abstract

Introduction: The alveolar bone is, like the remaining bones in the human organism, a labile structure that continues to remodel itself throughout one's life and plays a fundamental role in dental therapeutic approaches, such as in the placement of osseointegrated implants. There appears to exist some evidence that points towards the connection between hyperlipidaemia – a disease characterized by an imbalance between the circulating low-density lipoproteins and the high-density lipoproteins – and the altered bone metabolism, leading to osteopenia/osteoporosis. Bone marrow adipocytes produce large amounts of fatty acids, especially palmitic acid, which may display a local modulatory activity. Besides, this fatty acid is particularly abundant in bone marrow from patients diagnosed with osteoporosis, suggesting that it may have a role in the pathogenesis of this condition.

Objective: This study aims to address the biological effects of palmitic acid, at different concentrations, in the bone development process, in an embryonic chick femoral *ex vivo* model.

Methodology: Fertilized chick eggs were sacrificed at day 11. The femora were isolated and cultured in the air/liquid interface with medium containing bovine serum albumin and palmitic acid at 0, 50, 200 and 500 μM concentrations, for 11 days. Samples were characterized by microtomography and the morphological analysis was carried out to evaluate parameters as tissue volume, bone volume, tissue surface, bone surface and the bone mineral density. Samples were following characterized by histological assessment, with Alcian blue and Sirius red histochemical staining.

Results: Microtomographic analysis revealed that samples grown in the presence of 50 and 200 μM of palmitic acid exhibited an increased calcified sagittal section, as well as a thicker and more trabeculated transversal section, as compared to control and the 500 μM of palmitic acid. In addition, the 200 μM of palmitic acid condition exhibited significantly higher histomorphometric indexes. Histochemical analysis revealed no significant tissue organizational

differences between conditions, whether a thicker osteoid was verified for the 200 μM of palmitic acid condition.

Conclusion: Gathered evidence suggests that palmitic acid may be deposited in the embryonic femur organotypic model, and that mild and intermediate concentrations (50-200 μM) may stimulate the bone remodelling/growth cycle. Attained data indicates that the exposure to fatty acid may modify osteoblasts' functionality and induce morphological alterations and alter bone deposition and calcification. Therefore, the present work suggests that the biological functionality of the bone tissue in hyperlipidaemic conditions may lead to structural and functional differences on the tissue's architecture and have a clinically relevant impact on bone functionality.

Keywords: Fatty acids; Palmitic acid; Osteoblast; Osteoclast; Bone turnover; Osteopenia; Osteoporosis; Bone mineralization.

Resumo

Introdução: O osso alveolar é, à semelhança dos restantes ossos do corpo humano, uma estrutura lábil que permanece em remodelação ao longo da vida e que desempenha um papel fundamental de suporte e na efetivação de diferentes abordagens terapêuticas médico-dentárias, como a colocação de implantes osteointegrados. Existem indícios que apontam para uma conexão entre a hiperlipidemia (uma doença caracterizada pelo desequilíbrio entre as lipoproteínas de baixa e alta densidades, circulantes) e o metabolismo ósseo desregulado, o que poderá levar, em última instância à osteopenia/osteoporose. Os adipócitos da medula óssea produzem grandes quantidades de ácidos gordos, especialmente de ácido palmítico, que poderá exercer uma função reguladora local. Além disso, este ácido gordo é particularmente abundante na medula óssea de doentes com osteoporose, o que sugere uma ligação uma ligação entre este ácido gordo e a etiologia desta patologia.

Objetivo: O objetivo deste estudo assenta na avaliação dos efeitos biológicos do ácido palmítico, em diferentes concentrações, no processo de desenvolvimento ósseo, num modelo *ex vivo* de fémur de galinha embrionária.

Metodologia: Ovos de galinha fecundados foram sacrificados ao 11º dia de desenvolvimento embrionário. Os fémures foram isolados e cultivados numa interface ar/líquido num meio de cultura com ácido palmítico, nas concentrações de 0, 50, 200 e 500 μM, por 11 dias. As amostras foram estudadas através de microtomografia e de análise histológica, com o objetivo de avaliar parâmetros como o volume de tecido total, o volume ósseo, a superfície de tecido total, a superfície do osso e a densidade mineral óssea. As amostras foram, posteriormente, caracterizadas através de técnicas histológicas, com os corantes histoquímicos Alcian blue e Sirius red.

Resultados: A análise microtomográfica revelou que as amostras que cresceram na presença de ácido palmítico nas concentrações de 50 e de 200 μM apresentaram uma secção sagital mais calcificada, assim como uma secção transversal mais espessa e trabeculada, comparativamente às amostras que cresceram nas condições controlo, ou na presença de ácido palmítico a 500 μM.

Além disso, a condição dos 200 μM de ácido palmítico apresentou índices histomorfométricos mais elevados, com diferenças estatisticamente significativas, comparativamente à condição de controlo. A análise histoquímica não revelou diferenças significativas relativamente à organização do tecido entre as várias condições, exceto na condição de 200 μM, em que se observou uma matriz osteóide mais espessa.

Conclusão: As evidências recolhidas sugerem que o ácido palmítico se possa ter depositado no modelo organotípico de fémur embrionário e que, em concentrações baixas a intermédias (50-200 μM) possa estimular o ciclo de crescimento e remodelação óssea. Os dados obtidos indicam que a exposição ao ácido gordo poderá modificar a funcionalidade dos osteoblastos e induzir alterações morfológicas, o que se irá traduzir numa alteração na deposição óssea e na sua calcificação. Assim, este trabalho sugere que a funcionalidade biológica do tecido ósseo em condições hiperlipidémicas poder apresentar diferenças estruturais e funcionais na arquitetura do tecido, o que poderá ter um impacto clinicamente relevante na função óssea.

Palavras-chave: Ácidos gordos; Ácido palmítico; Osteoblasto; Osteoclasto; Renovação óssea; Osteopenia; Osteoporose; Mineralização óssea.

Table of Contents

List of Figures

List of Tables

List of Terms and Acronyms

Ca^{2+}	Calcium ion
PO_4^{3-}	Phosphate ion
Runx2	Runt-related transcription factor 2
Osx	Osterix
BMU	Bone multicellular unit
RANK	Receptor activator of nuclear factor κB
RANKL	RANK ligand
OPG	Osteoprotegerin
LRP5	Low-density lipoprotein receptor related protein 5
LRP6	Low-density lipoprotein receptor related protein 6
VLDL	Very low-density lipoprotein
IDL	Intermediate-density lipoprotein
LDL	Low-density lipoprotein
HDL	High-density lipoprotein
ACSL3	Long-chain acyl-CoA synthetase 3
USA	United States of America
PA	Palmitic acid
BSA	Bovine serum albumin
α-MEM	α-Minimal essential medium
dH_2O	Distilled water
DGAV	*Direção Geral da Alimentação e Veterinária*
µM	Micromolar
µCT	Microcomputed tomography scan
µm	Micrometre
µA	Microampere
ms	Milliseconds
TV	Tissue volume
BV	Bone volume
BV/TV	Bone volume and tissue volume ration
TS	Tissue surface
BS	Bone surface

BMD	Bone mineral density
IBM	International Business Machines
SPSS	Statistical Package for the Social Sciences

INTRODUCTION

1. Introduction

1.1 Bone

1.1.1 Bone constitution and function

It is well-known that the alveolar bone plays a fundamental role in dental therapeutic approaches, such as osseointegrated implants[1]. The alveolar bone is, like the remaining bones in the human organism, a labile structure that continues to remodel itself throughout one's life[1-3]. It is composed of a mineralized matrix and specialized cells that produce and maintain this same matrix. It consists of an organic component (osteoid) and a mineral component. The osteoid is made up specially of type I collagen, glycosaminoglycans and other proteins, while the inorganic bone matrix contains a highly substituted hydroxyapatite, with a generic chemical formulation of $(Ca_{10}[PO_4]_6[OH]_2)$[4].

The bone exhibits three different cell lines: the osteocytes, the osteoblasts and the osteoclasts. The osteocytes are flat cells found within the bone, in the lacunae[4-6]. They connect with one another through a complex series of canaliculi and control the calcium (Ca^{2+}) and phosphate (PO_4^{3-}) levels[4, 6]. These cells' death is followed by bone reabsorption[5, 6]. The osteoblasts are mesenchymal derived cells specialized in synthesizing, transporting and assembling the bone matrix along with regulating its mineralization[4]. These cells produce the organic component of the bone matrix by synthesizing many proteoglycans, glycoproteins and type I collagen. On the other hand, the bone matrix's mineralization is regulated by distinctive proteins, such as osteonectin (another osteoblast synthesized protein) which modulates Ca^{2+} deposition. Osteoblasts have also the ability to modulate other cell populations, through the production and release of osteocalcin into the blood stream. Osteoblasts deposit osteoid until they are fully trapped within. When this happens, osteoblasts enhance the mineralization process, becoming embedded into the mineralized matrix, becoming osteocytes[5, 7]. The osteoclasts are monocyte-derived specialized multinucleated cells responsible for reabsorbing bone and are usually found on the bone surface. The osteoclasts reabsorb bone by releasing acidic components and proteases into previously sealed locations (resorption pits/Howship lacunae), thus degrading inorganic and organic components[4, 5].

The bone's main functions are to provide a mechanical support, to ensure mineral homeostasis, to produce blood cells (via bone marrow), to protect the viscera and to transfer the forces generated by the muscles[4].

1.1.2 Bone physiology

During childhood and adolescence, the bone, including the alveolar section, goes under a phase of quick bone formation until it reaches its peak, being continuously associated with the remodelling process, needed to maintain the bone integrity and functionality[2, 4].

Bone formation may occur either through two different pathways, the intramembranous or the endochondral. The intramembranous pathway is mediated by mesenchymal stem cells differentiated into the osteoblastic lineage, while in the endochondral pathway, a transitory cartilage formation – formed by chondrocytes, occurs[4, 5, 8]. There are several transcription factors that determine the mesenchymal stem cell's fate, some of them being the runt-related transcription factor 2 (Runx2) and osterix (Osx). While Runx2 serves as a regulatory switch to form osteoblast precursor cells, Osx helps, not only to terminally differentiate the cells into the osteoblastic pathway, but also assisting on granting phenotypic features associated with the matrix formation and mineralization[8].

Bone remodelling is the name given to the process mediated by the conjoining activity of bone-reabsorbing cells (osteoclasts) and the bone-forming cells (osteoblasts)[2, 3, 6, 7, 9, 10]. This process begins with the establishment of a bone multicellular unit (BMU) formed by a group of osteoblasts and osteoclasts on the bone surface. All the events that occur in the BMU are regulated by cytokines and cell-cell interactions[4, 10].

The osteoclast signalling pathway of bone remodelling regulation includes receptor activator of nuclear factor κB (RANK) expressed on osteoclast precursors, the RANK ligand (RANKL) expressed on osteoblasts and marrow stromal cells and the osteoprotegerin (OPG) secreted by osteoblasts[4, 6, 8, 10-12]. When the RANK receptors are activated by the RANKL, the transcription factor NF-κB is activated. This is of vital importance for the differentiation from

osteoclast precursors into osteoclasts, and their subsequent survival. However, this process may be interrupted by the production of OPG, triggered by the binding of WNT proteins to the low-density lipoprotein receptor-related protein 5 (LRP5) and 6 (LRP6) receptors, on osteoblasts. The OPG molecule acts as a "decoy" receptor and binds to the RANKL, thus turning impossible its connection with RANK receptor, which will ultimately lead to a decreasing bone resorption[4, 6, 8, 10-12].

It is the balance between the RANK and the OPG activity that regulates both bone formation and resorption[4, 8, 10, 12]. Distinct factors can impair the stated equilibrium in bone formation/bone resorption, causing cellular dysfunction and abnormal bone deposition, ultimately leading to either bone fragility and/or fracture, or excessive bone density (for example osteopetrosis)[4, 6, 8-10].

1.2. Lipids

1.2.1. Biochemistry and biological role

Lipids are one of the many chemical compounds of food and, as such, they are divided into triglycerides, phospholipids and cholesterol. These substances are made of fatty acids, non-polar molecules composed of a long chain of hydrocarbons linked to a carboxylic acid functional group. The fatty acids more commonly present in the human body are either the stearic acid (18-carbon fully saturated chain), the oleic acid (18-carbon with one double bond in the middle of the chain) or the palmitic acid (16-carbon fully saturated chain)[13, 14]. Saturated chain is the name given to a single-bonded hydrocarbon chain while non-saturated chain is the denomination for chains which have a double bond somewhere in between the single bonds[13]. Usually, the three fatty acid chain molecules are united by one glycerol molecule, forming the triglyceride structure. Phospholipids are polar molecules composed of two fatty acid chains (one saturated and one non-saturated) and a phosphate group that is usually esterified to a polar amino compound[13]. Although cholesterol doesn't have fatty acids, it still retains the physical and chemical properties of other lipids[13, 14].

After being absorbed by the intestinal epithelium, the monoglycerides and fatty acids merge to form new triglycerides which enter the lymph as chylomicrons.

The chylomicrons are the least dense and the biggest of all the lipoproteins present in the blood stream[13]. Almost all the cholesterol and phospholipids that are absorbed also join the chylomicrons. The chylomicrons, then, enter the venous circulation at the junction of the jugular and subclavian veins. However, the chylomicrons do not last in the circulation as they are hydrolysed by the lipoprotein lipase, synthesized specially by the heart, the skeletal muscle and the adipose tissue, present in the surface of the endothelium. The fatty acids will diffuse into the adipose or muscle tissue and be either stored or used as fuel. The chylomicron remnants are then cleared from the blood stream[13, 14].

When the stored fatty acids are needed elsewhere in the human body, the triglycerides are hydrolysed into fatty acids and glycerol once again. Then, the fatty acids connect with serum albumin molecules and are distributed through the bloodstream. Fatty acids transported this way are called free fatty acids or non-esterified fatty acids[13-15]. During a post absorptive context, around 95% of all the lipids present in the blood stream are in the form of lipoproteins. These particles are smaller than the chylomicrons but have a similar composition. They can be divided into very low-density lipoproteins (VLDL), that present a high concentrations of triglycerides and moderate concentrations of cholesterol and phospholipids; intermediate-density lipoproteins (IDL), which are made from VLDL which cholesterol and phospholipids concentrations have risen because of the loss of some of the triglycerides; low-density lipoproteins (LDL), IDL that have lost all the triglycerides and thus have high cholesterol and phospholipid concentrations; and high-density lipoproteins (HDL), which are composed by around 50% of proteins and have a much reduced cholesterol and phospholipid concentration. VLDL's main task is to transport triglycerides from the liver mainly to the adipose tissue, while the remaining lipoproteins are used to transport cholesterol from the liver to the peripheral tissues (LDL) and backwords (HDL)[13, 14].

1.2.2. Hyperlipidaemia

Hyperlipidaemia is characterized by a disequilibrium between the LDL and the HDL in the blood stream[16]. It may be divided into two etiological entities: primary (familial) and secondary (acquired) hyperlipidaemia. The first type is caused by genetic disorders that the patient probably inherited from the progenitors. On the

other hand, the second type can be caused by many lifestyle connected factors such as an unhealthy diet, some medications (e.g. glucocorticoids or amiodarone), hypothyroidism or uncontrolled diabetes[17]. The major complication associated with hyperlipidaemia is atherosclerosis. This condition is caused by the accumulation of inner vase lesions called atheromas or atherosclerotic plaques. Atheromas are formed upon the interaction of distinct factors, including endothelium injury, inflammation and hyperlipidaemia, with the later playing a key role in this pathological cascade. Since the hyperlipidaemic patient's LDL concentration is much higher than that of the HDL, it is expected that the fatty acids' accumulation on endothelium will be more probable and, thus, favour atherosclerosis occurance[4, 14, 17].

There appears to exist some evidence that points towards the connection between hyperlipidaemia and altered bone metabolism, leading to osteopenia/osteoporosis[3, 18]. In fact, cholesterol stimulates osteoclastogenesis, thus decreasing the bone mass[18]. Therefore, cholesterol's lipoprotein regulation seems to be a key factor on what it counts to osteoclast differentiation. If the LDL concentration increases, so will cholesterol, and more osteoclasts will be formed and activated, promoting bone resorption. Osteopenia/osteoporosis will be more likely to occur. With the depletion of the LDL concentration (or the rising of the HDL), the opposite scenario will be more probable to happen[18]. Regarding the osteoblasts, some studies show that cholesterol inhibits both their proliferation and differentiation by reducing the expression of osteoblastic genes (such as Runx2) while others defend that cholesterol is a key factor in osteoblast differentiation through hedgehog-dependent and independent mechanisms[7]. In fact, cholesterol's role in osteoblast differentiation is rather complex and cannot be easily classified as either beneficial or deleterious[7] since it is not completely understood.

The marrow adipocytes produce large amounts of fatty acids, especially palmitic acid. Besides, this fatty acid is particularly abundant in bone marrow from patients diagnosed with osteoporosis, suggesting that it has a role in the pathogenesis of this illness[19]. On the other hand, this fatty acid seems to induce osteoblastic differentiation and bone mineralization by activating both long-chain acyl-CoA synthetase 3 (ACSL3) and NF-κB transcription factor[20]. It is also shown that fatty

acids share an important role in osteoblastogenesis as they are an important fuel source this whole process[2, 21].

1.3. Study models

Scientific development is highly dependent on experimentation models, such as *in vitro*, *ex vivo* and *in vivo* models. However, *in vitro* models rely on the use of a single or a low number of cell populations, and cannot perfectly mimic *in vivo* spatial arrangements or the native cell-cell or cell-matrix interactions[22]. The *in vivo* models, on the other hand, are expensive, demanding and broadly associated with ethical issues[22, 23]. To overcome all these adversities, *ex vivo* models have been developed, aiming to solve inherent limitations of both *in vitro* and *in vivo* systems. In this regard, the chick embryonic femora model has been established, allowing the characterization of the bone growth and development, on a native three-dimensional organization, mimicking the native biological interactions. Additionally, the *ex vivo* grown of this tissue in the absence of the immune response and accessibility for manipulation *in ovo,* further enhances experimental possibilities[23]. In this study's case, the immune cells' absence is extremely relevant since the osteoclasts are monocyte derived macrophages and, therefore, we can focus on studying hyperlipidaemia's impact on bone formation rather than bone resorption. The *ex vivo* embryonic chick long bone and limb bud models have been used to understand skeletal development for many years, with high translational data with *in vivo* settings[23].

1.4. Current scenario and aim of the study

In the United States of America (USA), roughly 53% of the adults have increased LDL levels, and therefore, hyperlipidaemia. These individuals exhibit a risk two times higher to develop cardiovascular diseases[16]. As said before, evidence linking the hyperlipidaemic condition and abnormal bone metabolism seems to be present, however, when it comes to hyperlipidaemia's impact on bone formation, it is difficult to find a conclusion as if higher cholesterol concentrations will stimulate or inhibit bone deposition[7]. As described before, palmitic acid is produced and stored by marrow adipocytes. Consequently, palmitic acid was the selected fatty acid for this study. For it to be soluble in the culture media, bovine

serum albumin (BSA) was added[24], since it mimics the physiological albumin transportation system[15].

Therefore, the aim of this study is to determine whether hyperlipidaemia influences the bone development process, in an embryonic chick femoral *ex vivo* model.

MATERIALS AND METHODS

2. Materials and Methods

2.1. Preparation of the culture media

The regular culture medium was compound by α-Minimal Essential Medium (α-MEM, Gibco, 11900-073) along with 1% (v/v) 2-phospho-L-ascorbic acid (Sigma-Aldrich, 49752-10G) and 1% penicillin/streptomycin (Gibco, 15240-062).

In order to obtain the experimental culture media, two stock solutions were prepared with and without palmitic acid (PA) (Sigma-Aldrich, P0500), using ethanol, bovine serum albumin (BSA, Sigma-Aldrich, A7906) and distilled water (dH_2O). In the first place, 140 mg of BSA were solubilized into 10 mL of dH_2O, while 51 mg of PA were solubilized into 1 mL of ethanol 100%. The BSA/dH_2O solution was filtered using a 0.2 µm filter (Sarstedt, 83.1826.102). This resulted into a 0.2 M PA solution and a 0.002 M BSA solution. The control stock solution was prepared by adding 0.25 mL of ethanol 100% to 4.75 mL of the BSA solution, while the hyperlipidaemic stock solution was prepared by adding 0.25 mL of the PA solution to 4.75 mL of the BSA solution (5:1 molar ratio[15]). Finally, different amounts of these stock solutions were added into the regular culture medium to achieve the hyperlipidaemic experimental media, as described in table I.

Table I. The detailed composition of hyperlipidaemic experimental media[19].

	Control Stock Solution	Hyperlipidaemic Stock Solution	Regular Medium (α-MEM)
C- (PA free)	50 µL	0 µL	950 µL
PA 50 µM	45 µL	5 µL	950 µL
PA 200 µM	30 µL	20 µL	950 µL
PA 500 µM	0 µL	50 µL	950 µL

2.2. Organotypic cultures of embryonic chick femora

All animal procedures were carried out in accordance with the local and national regulatory entity – *Direção Geral de Alimentação e Veterinária (DGAV)* and the Portuguese legislation regarding the technical standards of protection for experimental animals, according to both policies and principles of laboratory animal care and with the European Union guidelines (European Directive

2010/63/EU and National Decree-Law 113/2013). Fertilized chick eggs (*Gallus domesticus*) were kept at 37 ºC and 50% humidity in an incubator (Octagon Advance, Brinsea) and were later sacrificed at day 11 of incubation by decapitation. All the soft tissues were carefully removed, and the femora were completely dissected. The femora were then carefully positioned on Netwell® inserts (Costar 3480, 440 µm of pore diameter) placed into six-well plates (2 femora per well) along with 1 mL of regular culture medium. Femurs were grown at the air/liquid interface, with the culture media being changed once a day, for a total period of 11 days. After 6 days, femora were positioned on a graph paper, photographed and measured using ImageJ software, version 1.53c for Windows. Besides, the regular medium was replaced by medium containing PA at different concentrations (50 µM, 200 µM and 500 µM), along with the negative control (absent of PA). All the media were replaced once a day for the remaining 5 days. At the end of the experiment, femora were photographed and measured again and prepared for either histology or microtomographic evaluation. Femora samples were fixed with ethanol 70% for µCT scanning, or in 4% paraformaldehyde (PFA) for histochemical staining[25].

2.3. Microtomography evaluation (µCT)

Fixed samples were scanned at 40 kV, 100 µA, an exposure time of 800 ms and a voxel size of 4.5 µm using a Skyscan 1276 System (Brucker, version 1.0.11). The obtained projection images were reconstructed with the aid of NRecon software (Brucker, version 1.7.4.2) after setting the fine-tuning (ring reduction – 11, beam hardening – 40% and smoothening – 2) and the grayscale (0-0.18). Then, samples were aligned along the sagittal axis using DataViewer software (Brucker, version 1.5.6.2). The morphological analysis of the compact bone was carried out in between 900 slices (4 mm) from the centre of the diaphysis using CTAnalyser software (Brucker, version 1.17.7.2). The parameters calculated included were the tissue volume (TV), the bone volume (BV), the percentage of bone volume (BV/TV), the tissue surface (TS), the bone surface (BS), the bone surface/volume ratio (BS/BV), the bone surface density (BS/TV) and the bone mineral density (BMD). Three-dimensional images were generated using CTVox

software (Brucker, version 3.3.0)[26]. Four independent experiences were conducted.

2.4. Histological staining

The previously fixed femora were treated accordingly to Gruber et al. (2001)[27]. Samples were embedded in paraffin blocks that were later cut in 5 µm-thick sections. After rinsing in tap water for 10 minutes, the samples were stained in alcian blue solution, pH 2.5 (1 g alcian blue 8GX, Sigma-Aldrich, A-5268, CI 74240), 3 mL glacial acetic acid (Fisher) and 97 mL distilled water for 30 minutes at room temperature. Samples were, then, rinsed in tap water for 2 minutes and stained in picrosirius red solution (0.1 g sirius red F3B direct red, CI 35780, Sigma-Aldrich, 36554-8) mixed with 100 mL saturated aqueous picric acid, CI 10305 (Sigma-Aldrich, 925-40) for 1 hour at room temperature. After rinsing in 0.01 N HCl for 2 min, the specimens were dehydrated, cleared and mounted[27]. Images were captured using a Zeiss Axiolab 5 microscope coupled with an Axiocam 5 Colour Camera. Three independent experiments were performed**.** It is expected for the Sirius red solution to stain the collagenous matrix in red, while Alcian blue solution was used to stain the glycosaminoglycans in blue[25].

2.5. Statistical analysis

The statistical analysis was performed using the IBM SPSS program, version 27 for Windows (IBM Corp. Released 2020). The normality of the data was assessed using the Shapiro-Wilk test. For variables where normality was demonstrated, one-way ANOVA and Tukey's multiple comparison test or paired-samples T-test were used. On the other hand, for non-parametric datasets, Kruskal-Wallis or Wilcoxon tests were applied. The level of significance was set at $p < 0.05$ for all tests.

RESULTS

3. Results

In the present study, embryonic chick femora (E11) were cultured for 11 days in the air/culture medium interface, through *ex vivo* techniques. Grown femora revealed a great capability to undergo bone formation and growth processes, as shown by the following evidence.

3.1. Macroscopic Measurements

Grown femora were measured regarding length and thickness, at both the initial and final period of the *ex vivo* culture.

Regarding length, it is possible to understand that, although the differences are not statistically significant, there is a trend for reduced bone growth, proportional to the increase of the PA concentration (Fig. 1). Therefore, the more PA was present in the media, the less the bones grew in length.

Regarding bone thickness, a reduction of this measurement was verified for all experimental conditions grown in the presence of PA, in contrast to control. The decrease in thickness was not found to be concentration-dependent (Fig. 2).

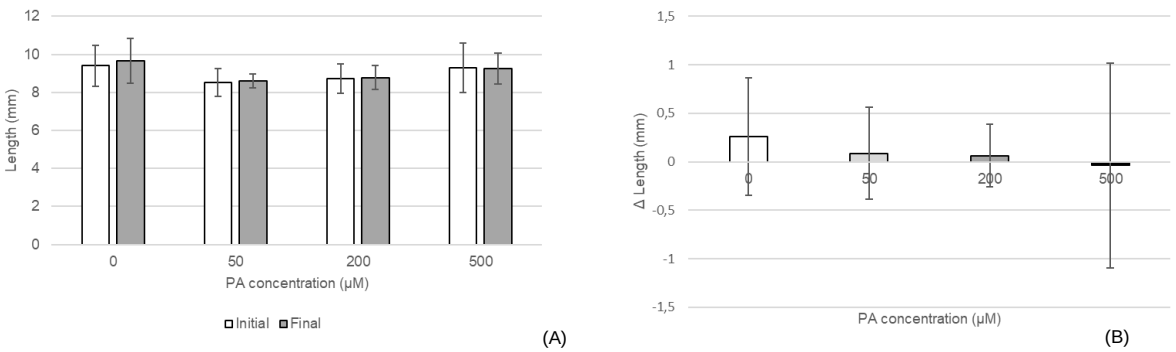

Figure 1. Length of the cultured femora. (A) Initial and final measurement of bones' length. Wilcoxon's test was carried to address potential correlations between the initial and final length, for each condition ($p>0,05$). (B) Length variation between the final and initial length measurement. Kruskal-Wallis' test was used to address potential differences on the Δ Length, between experimental conditions ($p>0,05$, see Attachments, tables III and V).

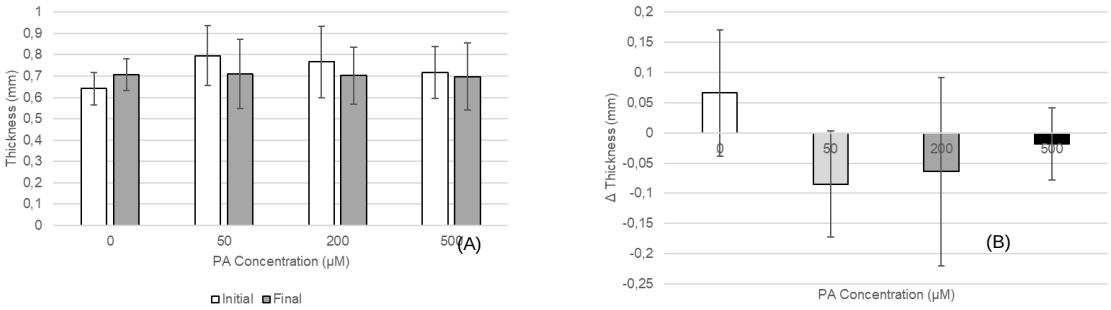

Figure 2. Thickness of the cultured femora. (A) Initial and final measurement of bones' length. Paired-Samples T-test was carried to address potential correlations between the initial and final thickness, for each condition (p>0,05). (B) Length variation between the final and initial length measurement. One-way ANOVA test was used to address potential differences on the Δ Thickness, between experimental conditions (p>0,05, (see Attachments, tables VII and IX).

3.2. Microtomographic evaluation (μCT)

Through macroscopical measurements, it is possible to acquire some information about the evolution and growth of the chick embryonic femora in *ex vivo* conditions. In addition, a microtomographic analysis assessment was performed in order to detail the morphometric parameters of the trabecular structure of the diaphysis. In the following table, data regarding some histomorphometric indexes are discriminated.

Table II. Microtomography measurements of organotypic cultured embryonic femora in regular medium and medium containing different concentrations of PA.

Sample	C- ($\bar{x}$ ± S)	50 μM ($\bar{x}$ ± S)	200 μM ($\bar{x}$ ± S)	500 μM ($\bar{x}$ ± S)
Tissue Volume (TV) / mm³	43.06 ± 3.51	31.69 ± 8.94	23.65 ± 6.80	27.57 ± 9.57
Bone Volume (BV) / mm³	0.30 ± 0.04	0.49 ± 0.09	0.52 ± 0.07	0.52 ± 0.18
BV/TV (%)	0.72 ± 0.14	1.64 ± 0.63	2.32 ± 0.70	1.96 ± 0.56
Tissue Surface (TS) / mm²	74.2 ± 10.3	63.44 ± 11.25	51.39 ± 9.16	56.13 ± 12.64
Bone Surface (BS) / mm²	11.02 ± 1.66	16.30 ± 2.43	24.70 ± 12.76	30.49 ± 19.48
BS/BV (1/mm)	35.86 ± 0.79	33.96 ± 7.47	46.30 ± 18.50	53.74 ± 19.83
BS/TV (1/mm)	0.28 ± 0.08	0.55 ± 0.21	1.01 ± 0.26	1.07 ± 0.61
Bone Mineral Density (BMD)	1	1.39 ± 0.63	1.77 ± 0.84	1.34 ± 0.32

Through a deep analysis of the microtomographic images (Fig. 3), it is possible to notice that the Control samples exhibited a small calcified diaphyseal section and a big epiphyseal area. Samples grown in the presence of 50 μM and 200 μM PA presented a longer calcified diaphyseal section, as well as a thicker and more

developed trabeculae transversal section when compared to control. Samples grown in the presence of 500 µM PA presented a mineralized diaphyseal section

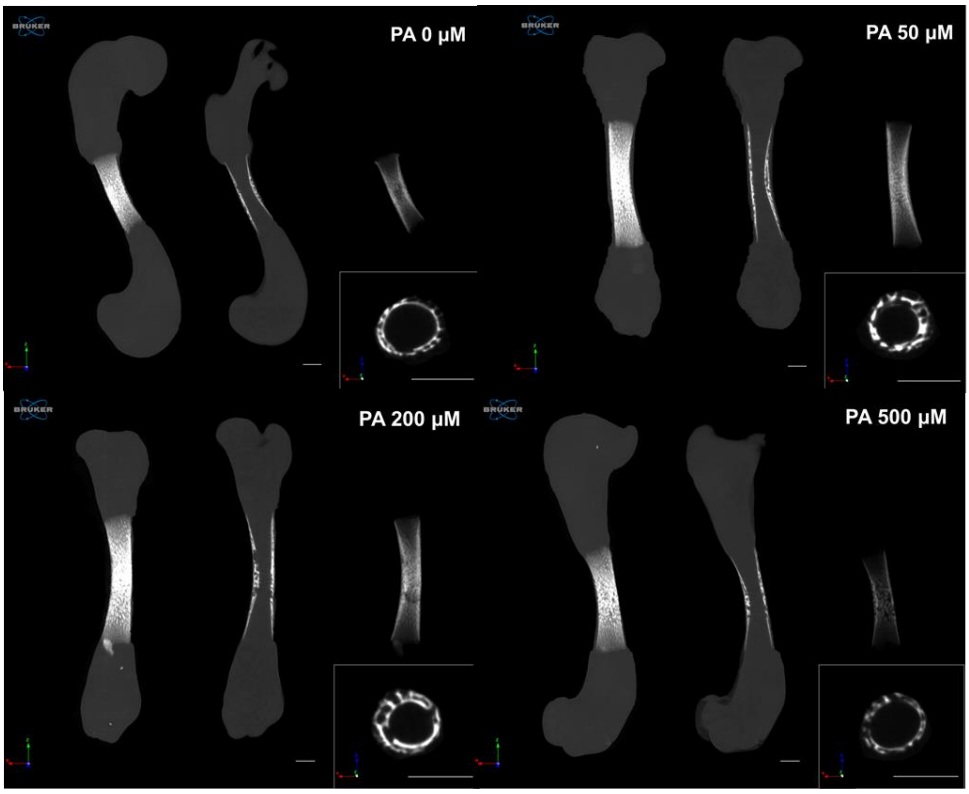

Figure 3. Representative images of the microtomographic reconstructions of femora grown in the distinct experimental conditions. Images from the left to the right, whole femur at maximum intensity projection, sagittal section, segmented mineralized bone and cross section of the central diaphysis region (n=4, scale 500 µm).

similar to control, that is, with a smaller and thinness calcified area. As in accordance with the macroscopic dimensional analysis, with the addition of PA, the femora growth tended to decrease, namely regarding thickness. However, a deeper study of both Tissue Volume and Bone Volume variables shows that, although the samples' growth rate depleted, they appear to exhibit an increased calcified portion when cultured with PA (Fig. 4A and 4B). In addition, bone surface was further found to have increased progressively (Fig.4E and Table II), with the increase of PA concentration.

In figure 4C it is observed the ratio of bone volume and tissue volume. Samples grown in the presence of PA presented values higher than control samples, attaining statistical significance at the 200 µM conditions. Among the experimental samples, 200 µM presented the highest values, followed by the 500 µM group. Therefore, by adding PA, it is possible to increase the ratio of calcified

tissue volume by the sample's total tissue volume. Interestingly, control samples presented a higher tissue volume and surface values, which can be correlated to the differences in size, observed in figures 1 and 2. Moreover, control samples presented the lowest amount of mineralized tissue, in alignment to figure 3.

Regarding the Bone Mineral Density, it seems that all the samples grown in the presence of PA show higher values than those of Control, with the highest values attained with the 200 μM concentration.

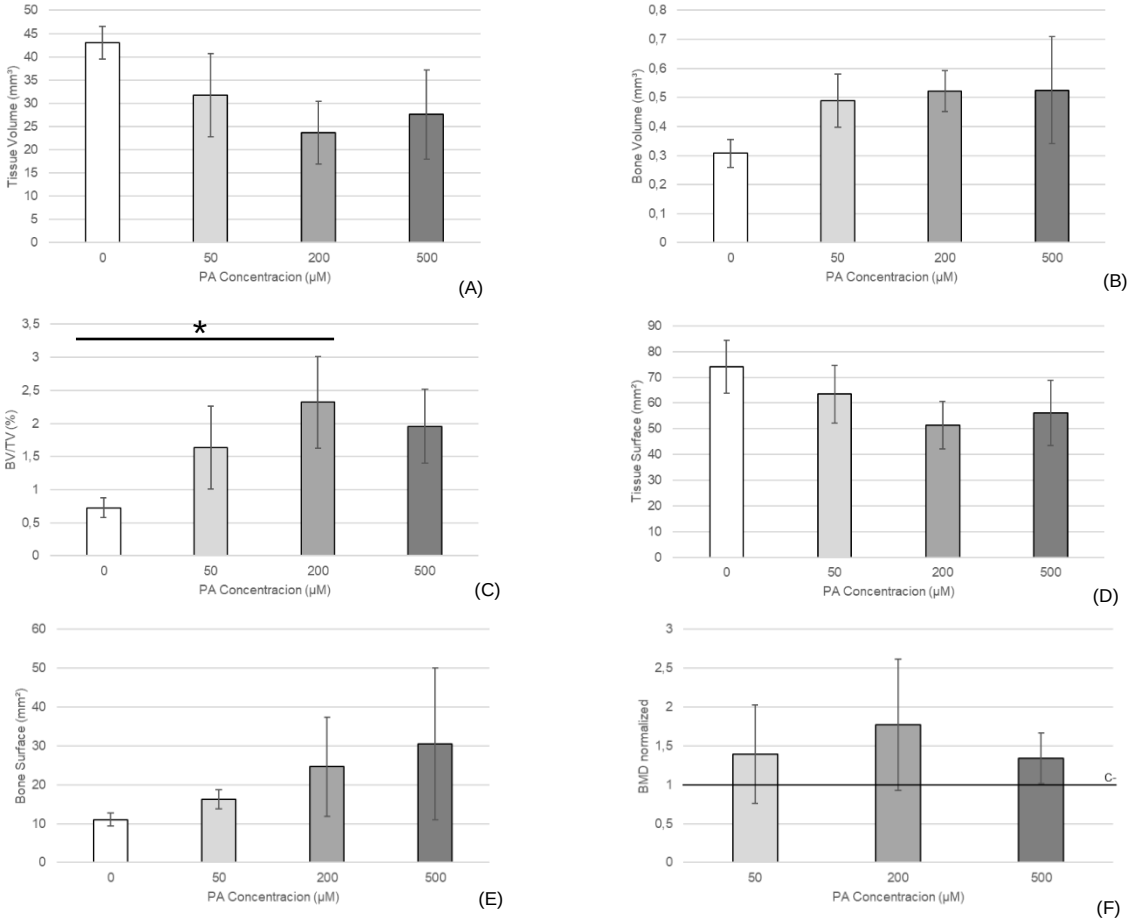

Figure 4. Microtomographic indexes. (A) Tissue Volume. (B) Bone Volume. (C) Division from Bone Volume to Tissue Volume (BV/TV). (D) Tissue Surface. (E) Bone Surface. (F) Normalized Bone Mineral Density. One-way ANOVA test was used in (A), (B), (C), (E) while Kruskal-Wallis' test was carried in (D) and (F). Control group's value is 1 since it has been normalized by this number (see Attachments, tables XI, XIII, XV, XVIII, XX and XXII).

*Control sample's differences are statistically significant from the 200 μM ($p<0.05$).

3.3. Histochemical staining

Regarding the histochemical analysis (Fig. 5), it is possible to observe the matrix's organization – the inner layer of the bone structure. The blue area, stained for the proteoglycan-rich matrix corresponds to cartilaginous tissue, stained by Alcian blue, while the surrounding layer was stained by Sirius red, showing the presence of collagen. No differences regarding the organization can be observed, however, 200 µM samples were shown to be the ones with the thickest collagen positive portion. The areas identified by the arrows in the 500 µM sample's show possible palmitic acid incorporation zones, due to differences in colour in comparison to control samples.

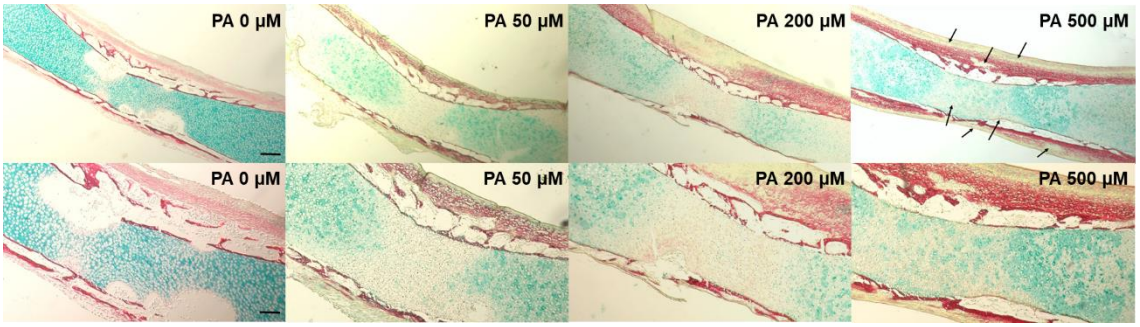

Figure 5. Histochemical staining with Alcian blue 8GX and Sirius red solutions for proteoglycans and collagen labelling, respectively. Scale bar corresponds to 100 µm for the upper portions and 200 µm for the lower portion of the image. Arrows point out a possible PA' incorporation into the tissues.

DISCUSSION

4. Discussion

As previously mentioned, lipids play an important role in bone turnover as they influence both the functionality of osteoclasts and osteoblasts[3, 18]. The influence of the lipid biomolecules on osteoclasts-related pathways is well studied and documented[18], while the modulation in osteoblasts-related pathways remains controversial[7]. Some studies suggest that the lipids represent a harmful factor that may inhibit osteoblast differentiation and proliferation[7]. On the other hand, other studies show that some lipidic components are key factors in osteoblast differentiation[7]. In the present study, PA was chosen due to fact that is the most prevalent fatty acid secreted by adipocytes[28].

In the obtained results, it is possible to understand from the macroscopic measurements that, with the gradual addition of PA, all samples manifested a tendency to both length and thickness reduction (Fig. 1 and 2). However, through microtomographic assessment, it was shown that the samples' calcified portion's ratio exhibited statistically significant differences (Fig. 4). In this context, the null hypothesis is rejected and, therefore, PA seems to influence positively the bone deposition since the samples displayed less non-calcified tissue (hence the length and thickness reduction) along with more and denser (higher bone mineral density values) calcified tissue. However, from one point onward, PA starts to present a negative influence rather than a positive one, as seen with the 500 µM group, throughout all the assessments. On what it counts to the histochemical staining, no major architecture changes were found besides the thicker calcified portion stained by the Sirius Red solution in the 200 µM group, which supports the idea that at high concentrations, PA may induce harmful effects on the osteoblastic functionality (Fig. 5). The probable PA incorporation sites may suggest higher osteoblast differentiation rates and, therefore, bone deposition in those specific places.

In vitro studies proved to be rather controversial as both harmful and beneficial outcomes could be demonstrated[7]. For instance, in the study of Gunaratnam et al. (2014), human osteoblasts cultured with 100 to 500 µM PA presented a significant reduction in differentiation, bone nodule formation and mineralization, including a significant reduction in the transcriptional activities of Runx2 – the

major osteogenic regulator transcription factor[28]. In addition, Kim et al. (2008) demonstrated that PA induced apoptosis in human osteoblasts by impairing the activation of Mitogen-activated protein kinase (MAPK/ERK), which contributes to the reduction in bone mineral density[29]. Further, osteoblasts cultured with 250 µM PA presented a dysfunctional autophagy and apoptosis, in the study of Saedi et al. (2020)[19]. On the other hand, some studies described positive effects in the presence of PA and other fatty acids on osteoblastic differentiation - the study of Rendina-Ruedy et al. (2017) found that bone marrow stromal cells cultured under osteogenic conditions presented intracellular lipid droplets and these droplets supported the osteoblast differentiation[2]. Furthermore, the study of Kageyama et al. (2013) described that PA can differentiate other cells into osteoblasts - vascular smooth muscle cells cultured with 250 µM of PA presented osteoblastic differentiation and mineralization by activating NF-κB signalling[20]. As described before in our results, mild cytotoxic effects were observed only at 500 µM of PA, suggesting that osteoblasts within the extracellular matrix can resist higher concentrations of PA in comparison to cellular monoculture. In addition, the 200 µM group presented higher mineral content, a concentration that is clearly cytotoxic for cultured osteoblasts.

In vivo studies suggest that higher PA levels may decrease circulating bone formation markers which affect osteoblast differentiation, as shown in Alsahli et al. (2015)[30]. In this study, male mice's diet was altered with growing fatty acid concentrations. Mice fed with higher PA concentrations, in their diets, displayed a diminished mineralization activity[30]. In addition, Muluke et al. (2016) had mice divided into 4 groups from which the fat percentage present in the diet of each group varied from one another. It was discovered that PA might accelerate bone loss through the enhancement of the inflammatory response in a periodontal disease obese mice model[31]. Being the *in vivo* models more complex and complete (i.e. presence of osteoclasts and potential systemic modulatory activities – as compared to the present *ex vivo* femur model), it is difficult to isolate the osteoblast's reaction from the complex *in vivo* response.

In this context, *ex vivo* studies proved to be of vital importance when variable control is needed without losing the 3D matrix architecture. Therefore, this study model may bring new insight into the detailed activity of PA on osteoblasts and

shed some light into new information of the potential modulatory activity of PA within the bone modelling, remodelling and regeneration.

CONCLUSION

5. Conclusion

The evidence gathered in this experimental work suggests that mild and intermediate PA concentrations (50 and 200 µM) may stimulate the bone remodelling cycle in the assayed *ex vivo* organotypic embryonic chick femora model. In addition, higher concentrations (500 µM) seem to induce deleterious effects, which indicates that the exposure to high PA levels may cause morphological alterations and compromise bone deposition and calcification, due to detrimental effects on osteoblasts' activity, aside from the increased osteoclastogenesis, described in the literature, within different models.

Therefore, the present work suggests that high hyperlipidaemic conditions may lead to bone fragility and bone development disruption. More studies are required to determine whether PA has a clinically relevant impact on bone functionality, as well as its potential modulation in the osteogenic differentiation process. Overall, the *ex vivo* organotypic embryonic chick femora study model proved to be a balanced alternative when compared to both *in vitro* and *in vivo* experimental models for studying hyperlipidaemic conditions.

BIBLIOGRAPHY

6. Bibliography

1. Monje A, Chan HL, Galindo-Moreno P, Elnayef B, Suarez-Lopez del Amo F, Wang F, et al. Alveolar Bone Architecture: A Systematic Review and Meta-Analysis. J Periodontol. 2015;86(11):1231-48.
2. Rendina-Ruedy E, Guntur AR, Rosen CJ. Intracellular lipid droplets support osteoblast function. Adipocyte. 2017;6(3):250-8.
3. Alekos NS, Moorer MC, Riddle RC. Dual Effects of Lipid Metabolism on Osteoblast Function. Front Endocrinol (Lausanne). 2020;11:578194.
4. Kumar V, Abbas AK, Aster JC. Robbins Basic Pathology. 10th ed: Elsevier Health Sciences; 2018.
5. Carneiro J, Junqueira LC. Histologia Básica - Texto & Atlas. 12th ed: Guanabara Koogan; 2013.
6. Kitaura H, Marahleh A, Ohori F, Noguchi T, Shen WR, Qi J, et al. Osteocyte-Related Cytokines Regulate Osteoclast Formation and Bone Resorption. Int J Mol Sci. 2020;21(14).
7. Yin W, Li Z, Zhang W. Modulation of Bone and Marrow Niche by Cholesterol. Nutrients. 2019;11(6).
8. Al-Bari AA, Al Mamun A. Current advances in regulation of bone homeostasis. FASEB Bioadv. 2020;2(11):668-79.
9. Lee WC, Guntur AR, Long F, Rosen CJ. Energy Metabolism of the Osteoblast: Implications for Osteoporosis. Endocr Rev. 2017;38(3):255-66.
10. Feng X, McDonald JM. Disorders of bone remodeling. Annu Rev Pathol. 2011;6:121-45.
11. Yang N, Liu D, Zhang X, Li J, Wang M, Xu T, et al. Effects of ginsenosides on bone remodelling for novel drug applications: a review. Chin Med. 2020;15:42.
12. Ming J, Cronin SJF, Penninger JM. Targeting the RANKL/RANK/OPG Axis for Cancer Therapy. Front Oncol. 2020;10:1283.
13. Baynes JW, Dominiczak MH. Medical Biochemistry. 4th ed: Elsevier Health Sciences; 2014.
14. Hall JE. Guyton and Hall Textbook of Medical Physiology. 13th ed: Elsevier Health Sciences; 2015.

15. Alsabeeh N, Chausse B, Kakimoto PA, Kowaltowski AJ, Shirihai O. Cell culture models of fatty acid overload: Problems and solutions. Biochim Biophys Acta Mol Cell Biol Lipids. 2018;1863(2):143-51.
16. Karr S. Epidemiology and management of hyperlipidemia. Am J Manag Care. 2017;23(9 Suppl):S139-s48.
17. Hill MF, Bordoni B. Hyperlipidemia. StatPearls. Treasure Island (FL): StatPearls Publishing Copyright © 2021, StatPearls Publishing LLC.; 2021.
18. Kim H, Oh B, Park-Min KH. Regulation of Osteoclast Differentiation and Activity by Lipid Metabolism. Cells. 2021;10(1).
19. Al Saedi A, C AG, D EM, Hayes A, Duque G. Rapamycin Affects Palmitate-Induced Lipotoxicity in Osteoblasts by Modulating Apoptosis and Autophagy. J Gerontol A Biol Sci Med Sci. 2020;75(1):58-63.
20. Kageyama A, Matsui H, Ohta M, Sambuichi K, Kawano H, Notsu T, et al. Palmitic acid induces osteoblastic differentiation in vascular smooth muscle cells through ACSL3 and NF-κB, novel targets of eicosapentaenoic acid. PLoS One. 2013;8(6):e68197.
21. Kushwaha P, Wolfgang MJ, Riddle RC. Fatty acid metabolism by the osteoblast. Bone. 2018;115:8-14.
22. Smith EL, Kanczler JM, Gothard D, Roberts CA, Wells JA, White LJ, et al. Evaluation of skeletal tissue repair, part 1: assessment of novel growth-factor-releasing hydrogels in an ex vivo chick femur defect model. Acta Biomater. 2014;10(10):4186-96.
23. Smith EL, Kanczler JM, Oreffo RO. A new take on an old story: chick limb organ culture for skeletal niche development and regenerative medicine evaluation. Eur Cell Mater. 2013;26:91-106; discussion
24. Manuel CR, Charron MJ, Ashby CR, Jr., Reznik SE. Saturated and unsaturated fatty acids differentially regulate in vitro and ex vivo placental antioxidant capacity. Am J Reprod Immunol. 2018;80(3):e12868.
25. Barros JAR, Melo LDR, Silva R, Ferraz MP, Azeredo J, Pinheiro VMC, et al. Encapsulated bacteriophages in alginate-nanohydroxyapatite hydrogel as a novel delivery system to prevent orthopedic implant-associated infections. Nanomedicine. 2020;24:102145.

26. Sousa DM, Martins PS, Leitão L, Alves CJ, Gomez-Lazaro M, Neto E, et al. The lack of neuropeptide Y-Y(1) receptor signaling modulates the chemical and mechanical properties of bone matrix. Faseb j. 2020;34(3):4163-77.
27. Gruber HE, Ingram J, Hanley EN, Jr. An improved staining method for intervertebral disc tissue. Biotech Histochem. 2002;77(2):81-3.
28. Gunaratnam K, Vidal C, Gimble JM, Duque G. Mechanisms of palmitate-induced lipotoxicity in human osteoblasts. Endocrinology. 2014;155(1):108-16.
29. Kim JE, Ahn MW, Baek SH, Lee IK, Kim YW, Kim JY, et al. AMPK activator, AICAR, inhibits palmitate-induced apoptosis in osteoblast. Bone. 2008;43(2):394-404.
30. Alsahli A, Kiefhaber K, Gold T, Muluke M, Jiang H, Cremers S, et al. Palmitic Acid Reduces Circulating Bone Formation Markers in Obese Animals and Impairs Osteoblast Activity via C16-Ceramide Accumulation. Calcif Tissue Int. 2016;98(5):511-9.
31. Muluke M, Gold T, Kiefhaber K, Al-Sahli A, Celenti R, Jiang H, et al. Diet-Induced Obesity and Its Differential Impact on Periodontal Bone Loss. J Dent Res. 2016;95(2):223-9.

ATTACHMENTS

7. Attachments

7.1. Data measurement tables

Table II. Shapiro-Wilk test for normality for the Δ Length variable.

Experimental		Kolmogorov-Smirnov[a]			Shapiro-Wilk		
		Statistic	df	Sig.	Statistic	df	Sig.
Δ Length	Control	0.274	6	0.180	0.811	6	0.073
	50 µM	0.238	6	0.200	0.928	6	0.566
	200 µM	0.216	6	0.200	0.937	6	0.632
	500 µM	0.360	6	0.015	0.748	6	0.019*

a. Lilliefors Significance Correction

Table III. Kruskal-Wallis test for the Δ Length variable.

	BMD
Kruskal-Wallis H	2.807
df	3
Asymp. Sig.	0.422

Table IV. Shapiro-Wilk test for normality for both Initial and Final Length variables.

Experimental		Kolmogorov-Smirnov[a]			Shapiro-Wilk		
		Statistic	df	Sig.	Statistic	df	Sig.
Initial Length	Control	0.143	6	0.200	0.965	6	0.858
	50 µM	0.348	6	0.022	0.765	6	0.028*
	200 µM	0.291	6	0.123	0.832	6	0.112
	500 µM	0.174	6	0.200	0.965	6	0.858
Final Length	Control	0.180	6	0.200	0.965	6	0.858
	50 µM	0.235	6	0.200	0.926	6	0.549
	200 µM	0.252	6	0.200	0.850	6	0.158
	500 µM	0.325	6	0.046	0.854	6	0.170

a. Lilliefors Significance Correction

Table V. Wilcoxon test for the Initial and Final Length variables.

	Final Length - Initial Length
Z	-0.371[b]
Asymp. Sig. (2-tailed)	0.710

a. Wilcoxon Signed Ranks Test
b. Based on negative ranks

Table VI. Shapiro-Wilk test for normality for the Δ Thickness variable.

Experimental		Kolmogorov-Smirnov[a]			Shapiro-Wilk		
		Statistic	df	Sig.	Statistic	df	Sig.
Δ Thickness	Control	0.212	6	0.200	0.920	6	0.508
	50 μM	0.193	6	0.200	0.921	6	0.512
	200 μM	0.159	6	0.200	0.959	6	0.812
	500 μM	0.204	6	0.200	0.939	6	0.655

a. Lilliefors Significance Correction

Table VII. One-way ANOVA test for the Δ Thickness variable.

	Sum of Squares	df	Mean Square	F	Sig.
Between groups	0.081	3	0.027	2.295	0.109
Within groups	0.234	20	0.012		
Total	0.315	23			

Table VIII. Shapiro-Wilk test for normality for both Initial and Final Thickness variables.

Experimental		Kolmogorov-Smirnov[a]			Shapiro-Wilk		
		Statistic	df	Sig.	Statistic	df	Sig.
Initial Thickness	Control	0.218	6	0.200	0.859	6	0.186
	50 μM	0.204	6	0.200	0.875	6	0.248
	200 μM	0.263	6	0.200	0.820	6	0.089
	500 μM	0.181	6	0.200	0.956	6	0.792
Final Thickness	Control	0.273	6	0.183	0.855	6	0.173
	50 μM	0.235	6	0.200	0.957	6	0.799
	200 μM	0.209	6	0.200	0.968	6	0.879
	500 μM	0.195	6	0.200	0.971	6	0.901

a. Lilliefors Significance Correction

Table IX. Paired-Samples T-test for the Initial and Final Thickness variables.

	Paired Differences					t	df	Sig. (2-tailed)
	Mean	Std. Deviation	Std. Error Mean	95% Confidence Interval of the Difference				
				Lower	Upper			
Initial Thickness - Final Thickness	0.02533	0.11697	0.02388	-0.02406	0.07473	1.061	23	0.300

Table X. Shapiro-Wilk test for normality for the Tissue Volume variable.

Experimental		Kolmogorov-Smirnov[a]			Shapiro-Wilk		
		Statistic	df	Sig.	Statistic	df	Sig.
Bone Volume	Control	0.348	3	.	0.834	3	0.199
	50 µM	0.233	3	.	0.979	3	0.725
	200 µM	0.175	3	.	1.000	3	1.000
	500 µM	0.181	3	.	0.999	3	0.939

a. Lilliefors Significance Correction

Table XI. One-way ANOVA test for the Tissue Volume variable.

	Sum of Squares	df	Mean Square	F	Sig.
Between groups	0.96	3	0.032	2.636	0.121
Within groups	0.097	8	0.012		
Total	0.193	11			

Table XII. Shapiro-Wilk test for normality for the Bone Volume variable.

Experimental		Kolmogorov-Smirnov[a]			Shapiro-Wilk		
		Statistic	df	Sig.	Statistic	df	Sig.
Bone Volume	Control	0.348	3	.	0.834	3	0.199
	50 µM	0.233	3	.	0.979	3	0.725
	200 µM	0.175	3	.	1.000	3	1.000
	500 µM	0.181	3	.	0.999	3	0.939

a. Lilliefors Significance Correction

Table XIII. One-way ANOVA test for the Bone Volume variable.

	Sum of Squares	df	Mean Square	F	Sig.
Between groups	0.096	3	0.032	2.636	0.121
Within groups	0.097	8	0.012		
Total	0.193	11			

Table XIV. Shapiro-Wilk test for normality for the BV/TV variable.

Experimental		Kolmogorov-Smirnov[a]			Shapiro-Wilk		
		Statistic	df	Sig.	Statistic	df	Sig.
BV/TV	Control	0.184	3	.	0.999	3	0.927
	50 µM	0.293	3	.	0.922	3	0.459
	200 µM	0.365	3	.	0.798	3	0.109
	500 µM	0.175	3	.	1.000	3	0.990

a. Lilliefors Significance Correction

Table XV. One-way ANOVA test for the BV/TV variable.

	Sum of Squares	df	Mean Square	F	Sig.
Between groups	4.154	3	1.385	4.509	0.039*
Within groups	2.457	8	0.307		
Total	6.611	11			

Table XVI. Tukey test for the BV/TV variable.

(I) Experimental		Mean Difference (I-J)	Std. Error	Sig.	95% Confidence Interval	
					Lower Bound	Upper Bound
Control	50 µM	-0.90667	0.45248	0.263	-2.3557	0.5423
	200 µM	-1.58667*	0.45248	0.033	-3.0357	-0.1377
	500 µM	-1.22667	0.45248	0.100	-2.6757	0.2223
50 µM	Control	0.90667	0.45248	0.263	-0.5423	2.3557
	200 µM	-0.68000	0.45248	0.479	-2.1290	0.7690
	500 µM	-0.32000	0.45248	0.891	-1.7690	1.1290
200 µM	Control	1.58667*	0.45248	0.033	0.1377	3.0357
	50 µM	0.68000	0.45248	0.479	-0.7690	2.1290
	500 µM	0.36000	0.45248	0.855	-1.0890	1.8090
500 µM	Control	1.22667	0.45248	0.100	-0.2223	2.6757
	50 µM	0.32000	0.45248	0.891	-1.1290	1.7690
	200 µM	-0.36000	0.45248	0.855	-1.8090	1.0890

*. The mean difference is significant at the .05 level.

Table XVII. Shapiro-Wilk test for normality for the Tissue Surface variable.

Experimental		Kolmogorov-Smirnov[a]			Shapiro-Wilk		
		Statistic	df	Sig.	Statistic	df	Sig.
Tissue Surface	Control	0.378	3	.	0.766	3	0.036*
	50 µM	0.341	3	.	0.847	3	0.233
	200 µM	0.221	3	.	0.986	3	0.772
	500 µM	0.216	3	.	0.989	3	0.795

a. Lilliefors Significance Correction

Table XVIII. Kruskal-Wallis test for the Tissue Surface variable.

	Tissue Surface
Kruskal-Wallis H	5.564
df	3
Asymp. Sig.	0.135

Table XIX. Shapiro-Wilk test for normality for the Bone Surface variable.

Experimental		Kolmogorov-Smirnov[a]			Shapiro-Wilk		
		Statistic	df	Sig.	Statistic	df	Sig.
Bone Surface	Control	0.337	3	.	0.855	3	0.254
	50 µM	0.318	3	.	0.886	3	0.343
	200 µM	0.330	3	.	0.867	3	0.286
	500 µM	0.176	3	.	1.000	3	0.986

a. Lilliefors Significance Correction

Table XX. One-way ANOVA test for the Bone Surface variable.

	Sum of Squares	df	Mean Square	F	Sig.
Between groups	674.184	3	224.728	1.631	0.258
Within groups	1102.191	8	137.774		
Total	1776.374	11			

Table XXI. Shapiro-Wilk test for normality for the Bone Mineral Density variable.

Experimental		Kolmogorov-Smirnov[a]			Shapiro-Wilk		
		Statistic	df	Sig.	Statistic	df	Sig.
Bone Mineral Density	Control	.	3	.	.	3	.
	50 µM	0.361	3	.	0.807	3	0.131
	200 µM	0.372	3	.	0.783	3	0.073
	500 µM	0.381	3	.	0.760	3	0.021*

a. Lilliefors Significance Correction

Table XXII. Kruskal-Wallis test for the Bone Mineral Density variable.

	BMD
Kruskal-Wallis H	3.979
df	3
Asymp. Sig.	0.264

7.2. Author's statement

U.PORTO
FACULDADE DE MEDICINA DENTARIA
UNIVERSIDADE DO PORTO

DECLARAÇÃO

Monografia/Relatório de Estágio

Declaro que o presente trabalho, no âmbito da Monografia/Relatório de Estágio, integrado no MIMD, da FMDUP, é da minha autoria e todas as fontes foram devidamente referenciadas.

19/05/2021

João Gabriel Cardoso

O/A Estudante

7.3. Advisor's statement

U.PORTO
FACULDADE DE MEDICINA DENTÁRIA
UNIVERSIDADE DO PORTO

Informo que o Trabalho de Monografia/Relatório de Estágio desenvolvido pelo(a)

Estudante João Gabriel Teixeira Cardoso

com o título: Hypothyroidism's impact on bone remodelling and development: Assessment in the rat mice organotypic embryonic chick femora model

está de acordo com as regras estipuladas na FMDUP, foi por mim conferido e encontra-se em condições de ser apresentado em provas públicas.

19/05/2021

O(A) Orientador(a)/Coorientador(a)

7.4. Repository statement

U.PORTO
FACULDADE DE MEDICINA DENTARIA
UNIVERSIDADE DO PORTO

DECLARAÇÃO
Mestrado Integrado em Medicina Dentária

Monografia/Relatório de Estágio

Identificação do autor

Nome completo João Gabriel Teixeira Cardoso

N.º de identificação civil 15558242 N.º de estudante 201708486

Email institucional up201708486@edu.fmd.up.pt

Email alternativo tjgabriel4498@gmail.com Tlf/Tlm 964205523

Faculdade/Instituto Faculdade de Medicina Dentária da Universidade do Porto

Identificação da publicação

Dissertação de Mestrado Integrado (Monografia) ☒ Relatório de Estágio ☐

Titulocompleto

Hyperlipidaemia's impact on bone remodelling and development: Assessment in the ex vivo organotypic embryonic chick femora model

Orientador Pedro de Sousa Gomes

Coorientador

Palavras-chave ; ; ; ;

Autorizo a disponibilização imediata do texto integral no Repositório da U.Porto: X (x)

Não Autorizo a disponibilização imediata do texto integral no Repositório da U.Porto : (x)

Autorizo a disponibilização do texto integral no Repositório da U.Porto, com período de embargo, no prazo de:

6 Meses: ; 12 Meses: ; 18 Meses: ; 24 Meses: ; 36 Meses: ; 120 Meses: .

Justificação para a não autorização imediata

U.PORTO
FACULDADE DE MEDICINA DENTARIA
UNIVERSIDADE DO PORTO

Data 19 / 05 / 2021

Assinatura João Gabriel Cardoso